Current Optics and Photonics
Vol. 3, No. 2, April 2019, pp. 164-171
ISSN: 2508-7266(Print) / ISSN: 2508-7274(Online)
DOI: https://doi.org/10.3807/COPP.2019.3.2.164

Effects of Carrier Leakage on Photoluminescence Properties of GaN-based Light-emitting Diodes at Room Temperature

Jongseok Kim[1]*, Seungtaek Kim[1], HyungTae Kim[1], Won-Jin Choi[2], and Hyundon Jung[3]

[1]*Smart Manufacturing Technology Group, Korea Institute of Industrial Technology, Cheonan 31056, Korea*
[2]*RayIR Co., Ltd., Suwon 16506, Korea*
[3]*Etamax, Suwon 16650, Korea*

(Received November 7, 2018 : revised December 28, 2018 : accepted December 28, 2018)

Photoluminescence (PL) properties of GaN-based light-emitting diodes (LEDs) were analyzed to study the effects of carrier leakage on the luminescence properties at room temperature. The electrical leakage and PL properties were compared for LEDs showing leakages at forward bias and an LED with an intentional leakage path formed by connecting a parallel resistance of various values. The leakages at the forward bias, which could be observed from the current-voltage characteristics, resulted in an increase in the excitation laser power density for the maximum PL efficiency (ratio of PL intensity to excitation power) as well as a reduction in the PL intensity. The effect of carrier leakages on PL properties was similar to the change in PL properties owing to a reduction of the photovoltage by a reverse current since the direction of the carrier movement under photoexcitation is identical to that of the reverse current. Valid relations between PL properties and electrical properties were observed as the PL properties deteriorated with an increase in the carrier leakage. The results imply that the PL properties of LED chips can be an indicator of the electrical properties of LEDs.

Keywords : Light-emitting diodes, Photoluminescence, Carrier leakage, Optical inspection
OCIS codes : (230.3670) Light-emitting diodes; (250.5230) Photoluminescence; (310.6188) Spectral properties; (120.4630) Optical inspection

I. INTRODUCTION

High-quality GaN-based light-emitting diodes (LEDs) have been developed intensively and applied in many areas including illumination and displays for a few decades [1, 2]. In order to maintain high optical quality of the devices for photonic applications, the luminescence properties of LEDs have been evaluated as one of the most important issues in the LED industry. At manufacturing sites, the luminescence properties of LEDs that can be observed for inspection are photoluminescence (PL) and electroluminescence (EL), which are produced by photoexcitation using light-emitting devices and direct current injection, respectively. In general, PL has been employed to inspect and evaluate the quality of LED epiwafers before the fabrication process [3].

However, a good estimation of the optoelectronic properties at chip levels using the PL results of epiwafers has not been possible, even though they provide a lot of information on the diode structure and material quality [4]. Therefore, most manufacturers have employed chip probers to inspect properties at chip levels under current injection conditions after the chip fabrication process. However, as there have not been sufficient results to correlate the PL properties and electrical properties of LEDs, there still remain questions as to whether it is possible to employ PL measurements on LED chips or chipwafers to evaluate the optoelectronic properties before chip-probing tests. A few research groups studied the optical properties of LED chips and reported relations and possible similarities between PL and EL properties [5-8]. Masui *et al*. proposed an experimental technique for correlating PL and EL measurements for InGaN-based blue and green LEDs by employing the reverse

*Corresponding author: jongseok@kitech.re.kr, ORCID 0000-0002-5740-2452
Color versions of one or more of the figures in this paper are available online.

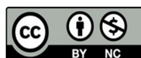
This is an Open Access article distributed under the terms of the Creative Commons Attribution Non-Commercial License (http://creativecommons.org/licenses/by-nc/4.0/) which permits unrestricted non-commercial use, distribution, and reproduction in any medium, provided the original work is properly cited.

Copyright © 2019 Current Optics and Photonics

saturation current under optical excitation to correlate with the forward current as the electrical excitation [5].

Li *et al*. reported on similarities in shape of PL and EL spectra and differences in peak positions and half-widths owing to junction temperature differences at identical injection intensities for AlGaInP-based red LEDs [6]. There were reports on correlations between PL and EL efficiency for InGaN LEDs [7, 8]. It was found that a change in EL efficiency as a function of the injection current density followed the trend of PL efficiency as a function of the excitation power density [7]. A difference between the trends of two efficiencies was discovered at very low excitation levels because of the different natures of the carrier generation processes for two excitation methods [8].

Regarding chips of low quality, Masui *et al*. mentioned that inferior chips showed weaker EL in the low-excitation level than PL owing to more significant leakage through leakage paths for the forward current than for the reverse case [5]. However, most of the reports showed comparisons between the EL and PL properties of typical LED chips with little degradation, and there have been few reports on the relation between photoexcitation and electrical excitation for LEDs with degraded properties.

In this study, we investigate the PL properties of LEDs, including chips with carrier leakage paths, in order to study the effects of electrical leakage on PL properties at room temperature and the relationship between the PL properties and some of the electrical properties. The purpose of this study is to examine PL properties that are effective in evaluating the electrical properties of LED chips in order to assess the possibility of PL measurements as an effective inspection method for LED chips or chip wafers. The results show a valid relation between the optical properties and electrical properties of LED chips by interlinking the PL properties and leakage properties of InGaN-based blue LEDs.

II. EXPERIMENTAL

Blue LEDs with a 455-nm emission wavelength, which were fabricated from a commercial 2-inch LED epiwafer with an InGaN-based multi-quantum well structure grown on sapphire substrate, were characterized. The chip size was 1200×700 μm^2. Diodes showing leakage current curves at forward bias from current-voltage (I-V) characteristics were selected to compare their PL properties. An LED chip showing a typical I-V characteristic with little leakage, R1, was selected as a reference chip. Two LED chips with different leakage properties, D1 and D2, were selected to examine the changes in PL properties owing to the leakage.

For comparison, we incorporated an intentional leakage path in LED R1 by connecting a resistance in parallel, and characterized the PL and electrical properties. Different values of resistance were connected one by one to establish different leakage levels. Photoluminescence measurements were performed using a micro-PL setup. For electrical characterization, we employed a sourcemeter connected to electrical contact probing modules attached to the wafer holder of the micro-PL setup for electrical characterization during measurements. A 405-nm resonant excitation laser beam with a 70-μm diameter was focused near the center of the LED chip under test. The excitation power was in the range of 0.1~100 mW, which corresponds to a power density in the range of 0.0026~2.6 kW/cm^2. We measured the luminescence spectra and intensities using a CCD-based spectrometer and a Si photodetector connected to a pico-ammeter.

III. RESULTS AND DISCUSSION

3.1. Electrical Characteristics of LED Chips

Figure 1(a) shows the I-V characteristics of three selected LED chips. Currents higher than 10^{-7} A were detected at a forward bias below 0.5 V for D1 and D2, which means that there are leakage paths in those two LEDs. As the EL began to be detected when the voltage was over 2.2 V for the samples, the leakage currents of the samples were measured just below the optical turn-on voltage for comparison. The currents at 2.2 V were 3.5×10^{-7} A, 1.5×10^{-5} A, and 6.5×10^{-4} A for R1, D1, and D2, respectively.

One of the important parameters for diodes, which is related to the carrier transport and recombination processes in the diode structures, is the ideality factor [9]. The ideality factor n can be obtained from Eq. (1), which can be derived from Eq. (2), the diode equation:

$$n = \frac{q}{k_B T}\left[\frac{\partial V}{\partial(\ln I)}\right] \tag{1}$$

$$I = I_0\left[\exp\left(\frac{qV}{nk_B T}\right) - 1\right] \tag{2}$$

where I_0 is the reverse saturation current, q is the elementary charge, k_B is the Boltzmann constant, and T is the absolute temperature [10, 11]. Figure 1(b) shows the ideality factors obtained from the I-V characteristics of the LED chips as a function of the forward voltage. As the voltage increased, the ideality factor decreased to the minimum value, and then increased owing to the series resistance in the high voltage region [10]. The minimum values of the ideality factors for the three selected LED chips were different from each other depending on the leakage current levels, as shown in the figure. As the slope of the currents determines the ideality factor [12], the ideality factor value increased in the region where the leakage process was dominant. The ideality factor can be an indicator of the forward leakage current, as a large leakage current results in a large ideality factor in a low-forward-bias region [13].

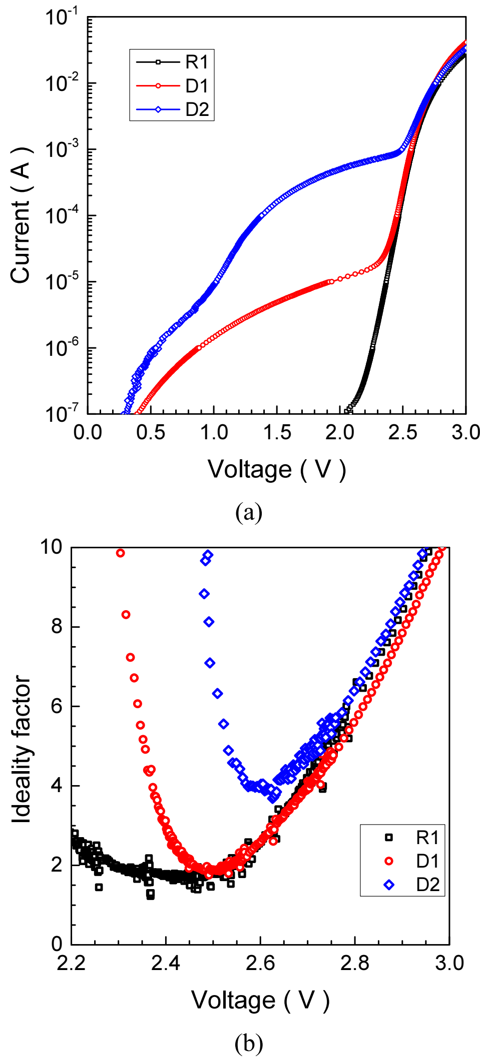

FIG. 1. Electrical properties of selected LEDs with different leakage properties: (a) I-V characteristics, (b) ideality factors obtained from I-V curves of LEDs with different leakage properties.

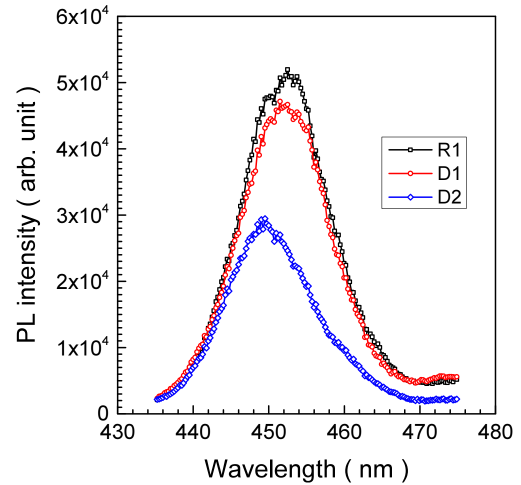

FIG. 2. PL spectra of LED chips with different leakage properties.

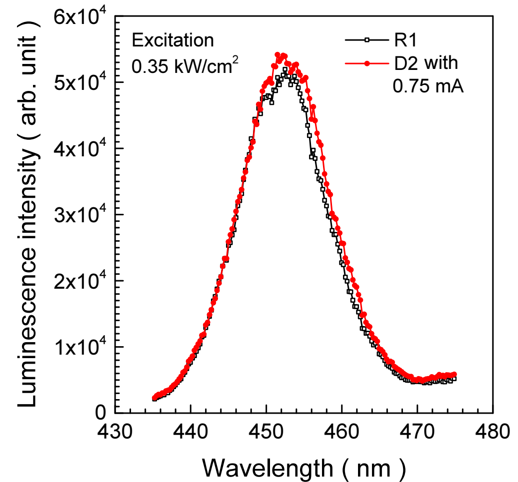

FIG. 3. Luminescence spectra of LED chips under photo-excitation of 0.35 kW/cm^2: PL spectrum of R1 (black square) and PL spectrum of D2 with additional EL by 0.75-mA current injection.

3.2. PL Properties of LED Chips

3.2.1. PL spectra of LEDs with leakages

We analyzed the PL properties of the three LED chips whose I-V properties were inspected in the previous section. The PL spectra of the samples obtained under an excitation power density of 0.35 kW/cm^2 are shown in Fig. 2. Under 0.35 kW/cm^2 of photoexcitation, the PL efficiency (ratio of PL intensity to excitation power) for LED R1, which showed little leakage, was at a maximum. At the excitation power used, the difference in the peak intensity between R1 and D1 was not large, while D2 showed quite a different spectrum with a low intensity of less than 60% compared to the other LEDs. The differences in the PL intensities of the LEDs imply that the PL intensity depends on the carrier leakage. The decrease in the intensity could be a result of leakage paths in samples D1 and D2.

When the carrier leakage was large, as for D2, in addition to a reduction in the PL intensity, the half-width of the spectrum was narrower than those of the others, which seems to result from the degradation of the luminescence in a long wavelength range. Under photoexcitation, we measured the open-circuit voltage (V_{OC}) by contacting the p- and n-electrodes of the LED. During photoexcitation in the open-circuit condition, parts of generated electrons and holes moved toward the n- and p-sides, respectively, and the accumulated carriers established V_{OC} [14]. V_{OC} for R1, D1, and D2 at the given laser power density of photo-excitation was 2.487 V, 2.479 V, and 2.138 V, respectively. V_{OC} for D2 was below the optical turn-on voltage for the LED emission, which was over 2.2 V. Schubert *et al.* found that EL could be induced with PL by photoexcitation in InGaN/GaN LEDs when the open-circuit voltage increased

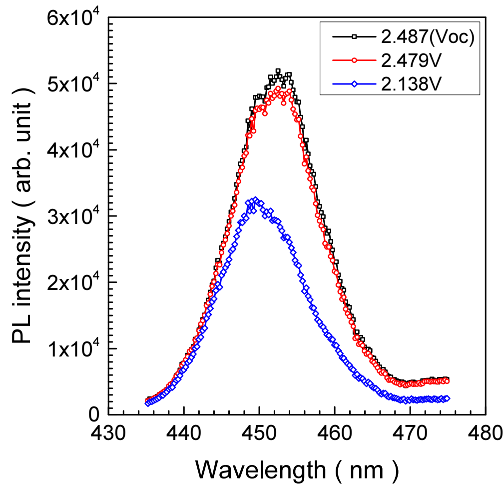

FIG. 4. PL spectra of LED R1 under different bias conditions obtained by reverse current flows (photoexcitation: 0.35 kW/cm^2).

beyond the optical turn-on voltage [15]. Referring to the results reported by Schubert *et al*. [15], EL could influence the luminescence spectrum when V_{OC} was over the optical turn-on voltage. Little EL was induced for D2 under the photoexcitation condition we used, which resulted in a narrow half-width owing to low intensity at longer wavelengths. When 0.75 mA of current injection was added to the photoexcitation for D2 to increase the V_{OC} value to the V_{OC} of R1 (2.487 V), the mixed luminescence spectrum of D2 became quite similar to the PL spectrum of R1, as shown in Fig. 3. The result implies that the injected current, which had a similar magnitude to the leakage current, counterbalanced the leakage current, and the LED operated as if there was little carrier leakage.

Thinking in the other direction, we investigated the PL spectra of R1 when the voltage under photoexcitation was reduced to 2.479 V and 2.138 V, which were the V_{OC} values of D1 and D2, respectively, by injecting reverse current. The spectra shown in Fig. 4 look very similar to Fig. 2, showing the PL spectra of D1 and D2 compared to R1. When the voltage between p- and n-sides of R1 was controlled to 2.479 V and 2.138 V, the current in the reverse direction was 3.8×10^{-5} A and 4.6×10^{-4} A, respectively. The magnitudes of the reverse currents were close to those of the leakage currents of D1 and D2, which indicates that the carrier leakage through the leakage paths of the LEDs at photoexcitation is a similar process to the reverse carrier flow, and results in a decrease of V_{OC}.

3.2.2. PL properties of LED chips depending on excitation laser power

We examined the excitation laser power dependence of the PL properties for the selected LED chips. The PL intensity of the samples increased with the excitation laser power, as shown in Fig. 5(a). The change in the PL intensity with respect to the excitation power is known to follow Eq. (3) [16]:

$$I_{PL} \propto P^S \tag{3}$$

where I_{PL} and P denote the PL intensity and excitation laser power, respectively. The S values for the samples were larger than 1 at low excitation levels and decreased with an increase in the excitation laser power, as shown in Fig. 5(b). The S values at low excitation levels for D2 were larger than those of R1, and the difference became smaller as the excitation power increased. This indicates a strong nonradiative process at a low excitation level for D2. When S is around 1, the radiative recombination is dominant, while an S around 2 implies that Shockley-Read-

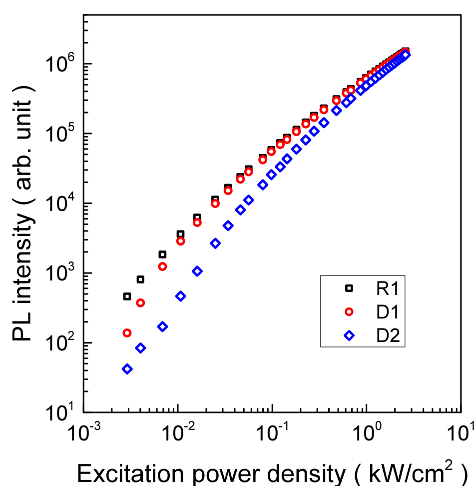

(a)

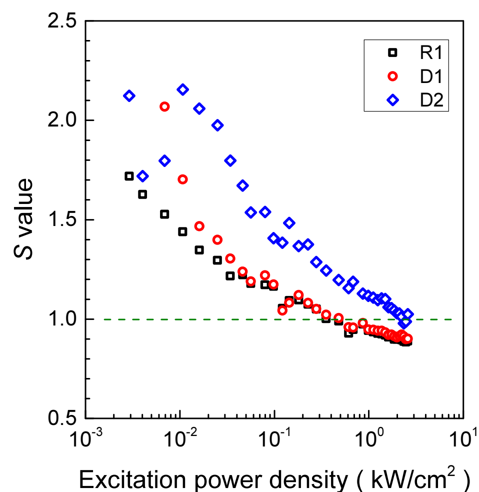

(b)

FIG. 5. (a) PL intensity as a function of excitation power density for LEDs with different leakages. (b) S values, obtained from PL intensity-excitation power curves, with respect to excitation power for LEDs with different leakages.

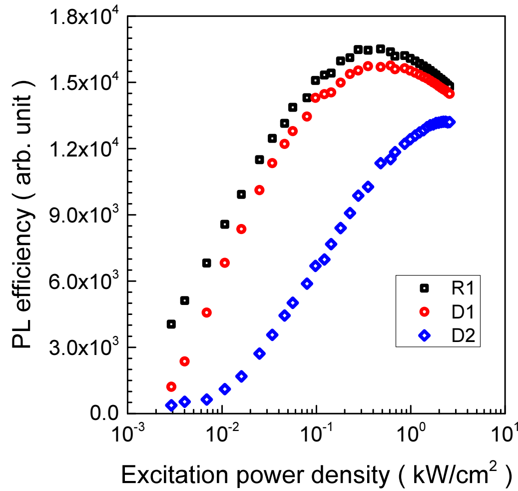

FIG. 6. PL efficiency with respect to excitation power for LEDs with different leakages.

Hall (SRH) nonradiative recombination is the major process. S is over 2 when other leakage processes are involved [17]. In most cases, the S values of LEDs are larger than 1 at low excitation levels whether the excitation method is electrical or optical, where nonradiative recombination is the dominant process [18]. Then, the value gets smaller as the excitation gets stronger. The excitation power level for $S = 1$ was higher for the LED with a higher leakage level, which indicates that more carrier generation is needed to compensate carrier losses through the leakage paths.

From the PL measurement, we obtained a PL efficiency by dividing the PL intensity by the excitation power (I_{PL}/P). The excitation power level where the PL efficiency is maximum, P_{max}, varies depending on the leakage level of the LEDs, as shown in Fig. 6. The P_{max} value implies the amount of carrier generation required to convert the dominant recombination process from nonradiative recombination to radiative recombination. The difference in P_{max} values for the chips could be a result of the difference in the excitation level where the recombination conversion from a nonradiative to radiative process occurs [19, 20]. The P_{max} values coincided with the excitation levels where the S value was 1, as shown for EL measurements [17], which indicates that the recombination process was mostly radiative at this point. P_{max} for R1, D1, and D2 was 13.9 mW (0.35 kW/cm^2), 18.8 mW (0.48 kW/cm^2), and 91.9 mW (2.34 kW/cm^2), respectively.

3.3. Effects of Parallel Resistance as Intentional Leakage Path

For LED structures, parallel parasitic resistances or degraded junctions are leakage paths that can be formed unintentionally during epitaxy or device fabrication processes [21]. In order to study the effect of leakages on PL properties for a wide range of leakage levels, we obtained the PL and electrical properties of LED R1 with a resistance

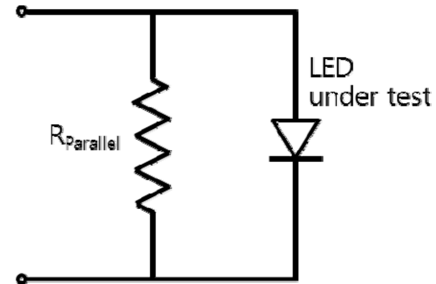

FIG. 7. Parallel resistance as a leakage path.

connected in parallel, as shown in Fig. 7, in addition to the properties of the selected LEDs. Resistances of 1 MΩ, 100 kΩ, 20 kΩ, 10 kΩ, and 5 kΩ were connected one by one for the measurements. The PL spectra of R1 with a parallel resistance ($R_{parallel}$) are shown in Fig. 8(a). The photoexcitation power density was 0.35 kW/cm^2 as we tested the selected LEDs. V_{OC} was reduced from 2.487 V to 2.486 V, 2.481 V, 2.455 V, 2.301 V, and 2.182 V as we added an $R_{parallel}$ of 1 MΩ, 100 kΩ, 20 kΩ, 10 kΩ, and 5 kΩ, respectively.

With a resistance under 10 kW, the leakage was so large that V_{OC} was reduced to under the optical turn-on voltage, and the spectrum peak wavelength blue-shifted with reduced intensity, which was observed in measurements for LED D2. The dependence of the PL efficiency on the excitation power for the LED with $R_{parallel}$ was obtained as shown in Fig. 8(b). The leakage currents at 2.2 V for the LED with resistances could be obtained from the I-V characteristics, which are shown in Fig. 8(c). This was consistent with the resistance values calculated using Ohm's law. Ideality factors calculated from the I-V characteristics using Eq. (1) are plotted in Fig. 8(d).

3.4. Relation between PL Properties and Electrical Properties

Figure 9(a) shows a reduction in PL intensity owing to carrier leakage. As the leakage level increased, the PL intensity decreased, and the slope changed slightly when the leakage current at 2.2 V was over 2×10^{-4} A, where V_{OC} from the PL measurement was under 2.3 V and the contribution of EL induced by spatially distributed carriers under photoexcitation was weakened [15]. Figure 9(b) shows the relation between P_{max} obtained from the PL efficiency analysis and the leakage level for selected LEDs and R1 with parallel resistances. As the carrier leakage level increased, a higher P_{max} was observed. The result indicates that more carrier generation by a higher photo-excitation level is needed to compensate the carrier leakages.

As we found from Figs. 1(b) and 8(d), the carrier leakage changes the ideality factor of the diode. Figure 9(c) shows the change in P_{max} with respect to the minimum ideality factor from Figs. 1(b) and 8(d), which was not different from the trend of change in P_{max} with respect to the degree of the carrier leakage.

FIG. 8. PL and electrical properties of a LED (R1) with parallel resistance of different values as an intentional leakage path: (a) PL spectra, (b) PL efficiency, (c) I-V characteristics, (d) ideality factors.

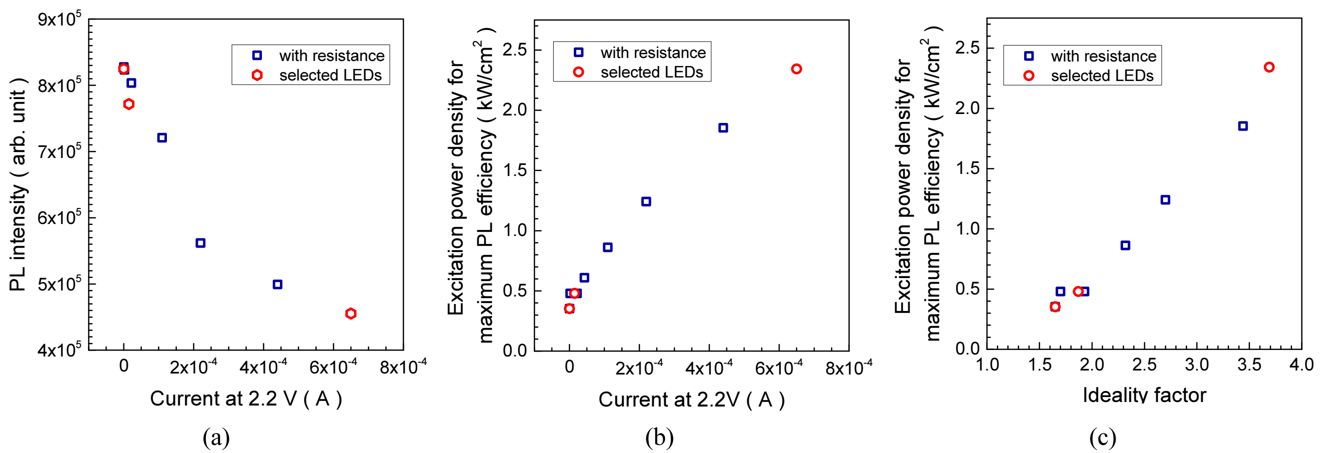

FIG. 9. Relations between PL properties and electrical properties: (a) PL intensity with respect to leakage current at 2.2 V of forward bias, (b) excitation power density for maximum PL efficiency (P_{max}) with respect to leakage current at 2.2 V of forward bias, (c) excitation power density for maximum PL efficiency with respect to ideality factor.

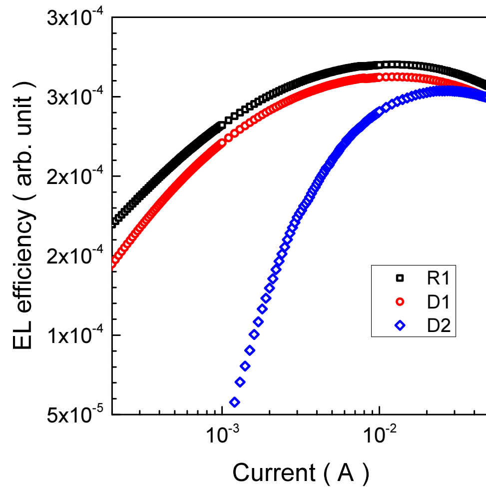

FIG. 10. EL efficiency with respect to injection current for LEDs with different leakages.

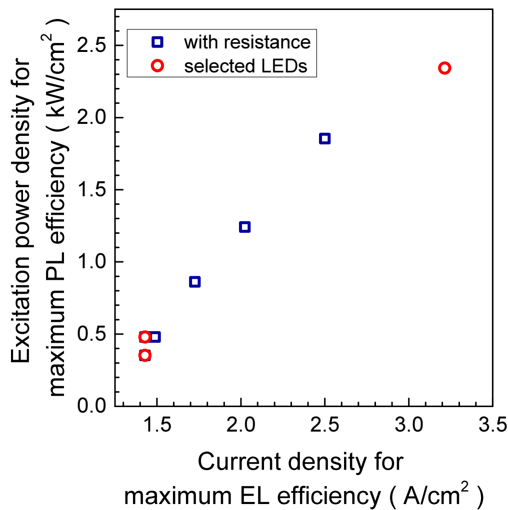

FIG. 11. Relation between excitation power density for maximum PL efficiency and current density for maximum EL efficiency.

We plotted the EL efficiencies (ratio of EL intensity to injection current) of the selected LEDs in Fig. 10. The overall shape of the plot was quite similar to the PL efficiency plot of Fig. 6. As EL efficiency can be proportional to the internal quantum efficiency [22], we can assess the quality of the LEDs with PL properties if the PL properties can be correlated with the EL properties. When we plotted a relation between J_{max}, the current density where the EL efficiency was maximum, and P_{max} for the selected LEDs and the LED with an intentional leakage path, we obtained the graph shown in Fig. 11.

The results show valid relations between the properties obtained under photoexcitation and electrical excitation for LED chips, which indicates that the PL properties of LED chips or chip wafers can be used to evaluate the electrical properties of the chips, particularly the leakage properties.

IV. SUMMARY

We studied the effects of the carrier leakage through leakage paths on the PL properties of InGaN-based LEDs. An LED with little leakage and two other LEDs with different leakage properties were analyzed, and results for an LED with an intentional leakage path were added. A reduced PL intensity and increase in the excitation level for maximum PL efficiency were observed for the LEDs with carrier leakages. The change in PL properties owing to carrier leakage was similar to the case of a reduced V_{OC} by a reverse current flow, which could result from the identical direction of the carrier flow of the photocurrent under photoexcitation and the reverse current. Carrier leakage during photoexcitation reduced V_{OC} as well as the PL intensity. A change in the decreasing rate of the PL intensity was observed at the point where V_{OC} decreased below the optical turn-on voltage, which implies that EL induced by photoexcitation could influence the luminescence property. In addition to the relation between the leakage currents and PL properties of LED chips, the ideality factors and J_{max} under a current injection condition could be correlated with P_{max} under a photoexcitation condition. The results showed that the PL properties of LED chips or chip-wafers can provide useful information when evaluating the electrical properties of LEDs at the chip level.

ACKNOWLEDGMENT

This work was supported by the Ministry of Trade, Industry, and Energy, Korea, under the Industrial Technology Innovation Program (Project No. 10067424).

REFERENCES

1. E. F. Schubert and J. K. Kim, “Solid-state light sources getting smart,” Science **308**, 1274-1278 (2005).
2. S. P. DenBaars, D. Feezell, K. Kelchner, S. Pimputkar, C.-C. Pan, C.-C. Yen, S. Tanaka, Y. Zhao, N. Pfaff, R. Farrell, M. Iza, S. Keller, U. Mishra, J. S. Speck, and S. Nakamura, “Development of gallium-nitride-based light-emitting diodes (LEDs) and laser diodes for energy-efficient lighting and displays,” Acta Mater. **61**, 945-951 (2013).
3. C. J. Raymond and Z. Li, “Photoluminescence metrology for LED characterization in high volume manufacturing,” Proc. SPIE **8681**, 86810P (2013).
4. Y. H. Aliyu, D. V. Morgan, and H. Thomas, “A luminescence mapping technique for rapid evaluation of visible-light-emitting materials used in semiconductor light-emitting diodes,” Meas. Sci. Technol. **8**, 437-440 (1997).
5. H. Masui, S. Nakamura, and S. P. DenBaars, “Experimental technique to correlate optical excitation intensities with electrical excitation intensities for semiconductor optoelectronic device characterization,” Semicond. Sci. Technol. **23**, 085108 (2008).

6. L. Li, P. Li, Y. Wen, J. Wen, and Y. Zhu, “Temperature dependences of photoluminescence and electroluminescence spectra in light-emitting diodes,” Appl. Phys. Lett. **94**, 261103 (2009).
7. A. Laubsch, M. Sabathil, J. Baur, M. Peter, and B. Hahn, “High-power and high-efficiency InGaN-based light emitters,” IEEE Trans. Electron Devices **57**, 79-87 (2010).
8. W.-A. Quitsch, D. Sager, M. Loewenich, T. Meyer, B. Hahn, and G. Bacher, “Low injection losses in InGaN/GaN LEDs: The correlation of photoluminescence, electroluminescence, and photocurrent measurements,” J. Appl. Phys. **123**, 214502 (2018).
9. H. Masui, “Diode ideality factor in modern light-emitting diodes,” Semicond. Sci. Technol. **26**, 075011 (2011).
10. J.-H. Ham, C.-H. Oh, D.-P. Han, H. Kim, J.-I. Shim, D.-S. Shin, and K.-S. Kim, “Study of the ideality factor of blue light-emitting diodes using the photovoltaic characteristics,” in *Proc. 11th Conference on Lasers and Electro-Optics Pacific Rim (CLEO-PR)* (Korea, Aug. 2015), 26P-106 (2015).
11. H.-J. Kim, G.-H. Ryu, W.-B. Yang, and H.-Y. Ryu, “Ideality factor of GaN-based light-emitting diodes determined by the measurement of photovoltaic characteristics,” J. Korean Phys. Soc. **65**, 1639-1643 (2014).
12. S. W. Lee, D. C. Oh, H. Goto, J. S. Ha, H. J. Lee, T. Hanada, M. W. Cho, T. Yao, S. K. Hong, H. Y. Lee, S. R. Cho, J. W. Choi, J. H. Choi, J. H. Jang, J. E. Shin, and J. S. Lee, “Origin of forward leakage current in GaN-based light-emitting devices,” Appl. Phys. Lett. **89**, 132117 (2006).
13. J. Kim, H. Kim, S. Kim, H. Jeong, I. Cho, M. Noh, H. Jung, and K. Jin, “Properties of defective regions observed by photoluminescence imaging for GaN-based light-emitting diode epi-wafers,” J. Opt. Soc. Korea **19**, 687-694 (2015).
14. S.-H. Lim, Y.-H. Ko, and Y.-H. Cho, “A quantitative method for determination of carrier escape efficiency in GaN-based light-emitting diodes: A comparison of open- and short-circuit photoluminescence,” Appl. Phys. Lett. **104**, 091104 (2014).
15. M. F. Schubert, Q. Dai, J. Xu, J. K. Kim, and E. F. Schubert, “Electroluminescence induced by photoluminescence excitation in GaInN/GaN light-emitting diodes,” Appl. Phys. Lett. **95**, 191105 (2009).
16. Y. Sun, H. Guo, L. Jin, Y.-H. Cho, E.-K. Suh, H. J. Lee, R. J. Choi, and Y. B. Hahn, “Optical excitation study on the efficiency droop behaviors of InGaN/GaN multiple-quantum-well structures,” Appl. Phys. B **114**, 551-555 (2014).
17. K.-S. Kim, D.-P. Han, H.-S. Kim, and J.-I. Shim, “Analysis of dominant carrier recombination mechanisms depending on injection current in InGaN green light emitting diodes,” Appl. Phys. Lett. **104**, 091110 (2014).
18. I. Mártil, E. Redondo, and A. Ojeda, “Influence of defects on the electrical and optical characteristics of blue light-emitting diodes based on III-V nitrides,” J. Appl. Phys. **81**, 2442 (1997).
19. T. Kohno, Y. Sudo, M. Yamauchi, K. Mitsui, H. Kudo, H. Okagawa, and Y. Yamada, “Internal quantum efficiency and nonradiative recombination rate in InGaN-based near-ultraviolet light-emitting diodes,” Jpn. J. Appl. Phys. **51**, 072102 (2012).
20. Q. Wang, Z.-W. Ji, F. Wang, Q. Mu, Y.-J. Zheng, X.-G. Xu, Y.-J. Lü, Z.-H. Feng, “Influence of excitation power and temperature on photoluminescence in phase-separated InGaN quantum wells,” Chin. Phys. B **24**, 024219 (2015).
21. E. F. Schubert, *Light-Emitting Diodes*, 2nd ed. (Cambridge University Press, Cambridge, UK, 2006), Chapter 4.
22. H. Masui, H. Sato, H. Asamizu, M. C. Schmidt, N. N. Fellows, S. Nakamura, and S. P. Denbaars, “Radiative recombination efficiency of InGaN-based light-emitting diodes evaluated at various temperatures and injection currents,” Jpn. J. Appl. Phys. **46**, L627-L629 (2007).